European Journal of Nuclear Medicine and Molecular Imaging (2022) 49:1322–1337
https://doi.org/10.1007/s00259-021-05576-w

ORIGINAL ARTICLE

Positron emission tomography and computed tomography with [^{68}Ga] Ga-fibroblast activation protein inhibitors improves tumor detection and staging in patients with pancreatic cancer

Yizhen Pang[1] · Long Zhao[1] · Qihang Shang[1] · Tinghua Meng[1] · Liang Zhao[2] · Liuxing Feng[3] · Shuangjia Wang[3] · Ping Guo[3] · Xiurong Wu[4] · Qin Lin[2] · Hua Wu[1] · Weipeng Huang[5] · Long Sun[1] · Haojun Chen[1]

Received: 1 August 2021 / Accepted: 24 September 2021 / Published online: 15 October 2021

Abstract

Purpose This study aimed to investigate the diagnostic performance of [^{68}Ga]Ga-FAPI PET/CT for primary and metastatic pancreatic carcinoma lesions and compare the results with those of [^{18}F]-fluorodeoxyglucose ([^{18}F]FDG) PET/CT.

Methods Patients with suspected or diagnosed pancreatic malignancy, who underwent contemporaneous [^{18}F]FDG and [^{68}Ga]Ga-FAPI PET/CT between June 2020 and January 2021, were retrospectively analyzed. Routine contrast-enhanced CT (CE-CT) is performed in all patients as standardized care. Findings were confirmed by histopathology or radiographic follow-up. We compared radiotracer uptake, diagnostic performance, and TNM (tumor-node-metastasis) classifications.

Results We evaluated 36 participants (25/36 men; median age, 60 years), including 26 patients with pancreatic malignancies and ten patients with pancreatic benign lesions. [^{68}Ga]Ga-FAPI PET/CT showed higher radiotracer uptake and higher sensitivity than [^{18}F]FDG PET/CT in evaluating primary tumors (SUVmax, 21.4 vs. 4.8; sensitivity, 100% vs. 73.1%), involved lymph nodes (SUVmax, 8.6 vs. 2.7; sensitivity, 81.8% vs. 59.1%), and metastases (SUVmax, 7.9 vs. 3.5; sensitivity, 91.5% vs. 44.0%); Compared with [^{18}F]FDG, [^{68}Ga]Ga-FAPI PET/CT upstaged six patients' TNM staging (6/23, 26.1%) and changed two patients' clinical management (2/23, 8.7%). Compared with CE-CT, [^{68}Ga]Ga-FAPI PET/CT upgraded TNM staging in five patients (5/23, 21.7%) and changed the therapeutic regimen in only one patient (1/23, 4.3%). Intense [^{68}Ga]Ga-FAPI uptake was observed throughout the pancreas in 12/26 pancreatic malignancies; dual-time point [^{68}Ga]Ga-FAPI PET/CT may differentiate pancreatitis from malignancy.

Conclusions Compared with [^{18}F]FDG PET/CT, [^{68}Ga]Ga-FAPI PET/CT shows higher sensitivity in detecting primary pancreatic tumors, involved lymph nodes, and metastases and is superior in terms of TNM staging. Prospective trials with larger patient population are needed to evaluate whether [^{68}Ga]Ga-FAPI PET/CT could elicit treatment modification in pancreatic cancer when compared with standard of care imaging.

Keywords [^{18}F]FDG · [^{68}Ga]Ga-FAPI · PET/CT · Pancreatic cancer

Introduction

Pancreatic cancer is a leading cause of cancer mortality worldwide, with a 5-year survival rate < 10% [1]. The only potentially curative therapy for pancreatic cancer is the combination of surgical resection and chemotherapy, but most patients with pancreatic cancer are diagnosed at an advanced stage (precluding the opportunity for resectable tumors) [2]. An optimal imaging modality is crucial for early diagnosis and accurate staging in patients with pancreatic cancer.

Contrast-enhanced CT (CE-CT) and magnetic resonance imaging (MRI) are widely recommended for diagnosing pancreatic cancer [3]. However, CE-CT often misses small

Yizhen Pang, Long Zhao and Qihang Shang contributed equally to this work.

This article is part of the Topical Collection on Oncology - General

✉ Weipeng Huang
jyhuangweipeng@vip.sina.com

✉ Long Sun
13178352662@163.com

✉ Haojun Chen
leochen0821@foxmail.com

Extended author information available on the last page of the article

pancreatic tumors (< 20 mm), small liver metastases, and peritoneal carcinoma [4]. MRI is superior to CE-CT in detecting small liver metastases due to its high resolution but is similarly sensitive and specific in evaluating pancreatic cancer. Additionally, MRI is limited in detecting distant metastases because of its screening range.

Although NCCN guideline does not recommend fluorine-18 ([^{18}F]) fluorodeoxyglucose (FDG) PET/CT as the first-line imaging modality for the diagnosis of pancreatic cancer [3], it may be considered in high-risk patients to detect extra-pancreatic metastases [5, 6]. However, owing to its limited sensitivity for detecting involved lymph nodes (30–49%), liver metastases (43–88%), and peritoneal carcinomatosis (42.9–60%), [^{18}F]FDG PET/CT is sometimes of limited use for surgical planning in pancreatic cancer [7–9]. Thus, it is necessary to explore a more effective imaging technique for pancreatic tumor detection and staging.

Gallium 68 ([^{68}Ga]Ga)-labeled fibroblast activation protein inhibitor (FAPI) is a novel PET tracer that targets fibroblast activation proteins (FAP) expressed on cancer-associated fibroblasts (CAFs) [10, 11]. Recently, [^{68}Ga]Ga-FAPI PET/CT has been successfully applied to imaging various types of tumors [12–14]. Pancreatic tumors are characterized by intense stromal desmoplastic reactions surrounding cancer cells, and CAFs are the main effector cells in the desmoplastic reaction [15]. Therefore, pancreatic cancer is expected to show intensive uptake of [^{68}Ga]Ga-FAPI [12], and previous studies have demonstrated good potential clinical value of [^{68}Ga]Ga-FAPI PET/CT for the diagnosis of pancreatic cancer [13, 16]. Herein, we further explored the diagnostic efficacy of [^{68}Ga]Ga-FAPI PET/CT for the primary and metastatic pancreatic cancer and compare the results with those of [^{18}F]FDG PET/CT.

Materials and methods

Demographic and medical characteristics

This is a post hoc retrospective analysis of a sub-cohort of patients from a previously prospectively acquired database, namely the patient data screened in a study that was registered at ClinicalTrials.gov (NCT04416165) and was approved by the Clinical Research Ethics Committee of the First Affiliated Hospital of Xiamen University (ID 2020-KY042). With agreement from the oncologists and on determination of the patients' eligibility, patients were recruited for enrolment in the study, from June 2020 through January 2021, at our institute. All participants provided written informed consent. The time interval between [^{18}F]FDG and [^{68}Ga]Ga-FAPI PET/CT was 1–6 days. Inclusion criteria were as follows: (i) patients undergoing paired [^{18}F]FDG and [^{68}Ga]Ga-FAPI PET/CT for discriminating pancreatic mass lesions, (ii) patients undergoing paired [^{18}F]FDG and [^{68}Ga]Ga-FAPI PET/CT for tumor staging, and (iii) patients who were able to provide informed consent and permission according to the Clinical Research Ethics Committee guidelines. Exclusion criteria were as follows: (i) pregnancy, (ii) start of treatment before [^{68}Ga]Ga-FAPI PET/CT scan, and (iii) inability or unwillingness of the research participant or legal representative to provide written informed consent. Histopathology served as the gold standard for final diagnosis. For cases in which tissue diagnosis was not applicable, radiographic follow-up was requested. The minimal follow-up period was 3 months. Lesions were considered malignant during follow-up based on (i) typical malignant features confirmed by multimodality medical imaging (including CT, MRI, and ultrasound), (ii) significant progression on follow-up imaging (define by the significant increase in size), and (iii) a substantial reduction in size after anti-cancer treatment (chemotherapy, radiotherapy, targeted therapy). The radiographic follow-up data was presented in Supplemental material.

Synthesis of radiopharmaceuticals

[^{18}F]FDG was routinely synthesized at the Minnan PET Center of the First Affiliated Hospital, following standard methodology [17]. The FAPI precursor (DOTA-FAPI-04) was purchased from CSBio Ltd. (Shanghai, China). Radiolabeling of [^{68}Ga]Ga-FAPI was conducted according to a previously described protocol [13]. The final product was diluted with saline and sterilized by passing through a 0.22-μm Millipore filter (EMD Millipore, Billerica, MA) into a sterile multidose syringe; radiochemical purity was > 95% for both [^{18}F]FDG and [^{68}Ga]Ga-FAPI. Sterility tests were performed in-house at the radiochemistry facility of the hospital; [^{68}Ga]Ga-FAPI and [^{18}F]FDG tracers met all standard criteria before human administration.

Image acquisition and processing

All patients underwent sequential [^{18}F]FDG and [^{68}Ga]Ga-FAPI PET/CT scanning within 1 week. [^{18}F]FDG PET/CT was conducted after > 6 h of fasting and among patients with normal blood glucose levels. No specific preparation was required for [^{68}Ga]Ga-FAPI PET/CT. Radioactivity doses of injected [^{18}F]FDG and [^{68}Ga]Ga-FAPI were calculated according to patients' weights (3.7 MBq [0.1 mCi]/kg for FDG; 1.8–2.2 MBq [0.05–0.06 mCi]/kg for FAPI). Static PET/CT imaging was performed using a hybrid PET/CT system (Discovery MI, GE Healthcare, Milwaukee, WI, USA) 60 min after injection. PET/CT scan was performed from the skull base to upper thigh (for [^{18}F]FDG, the head scan was performed separately) or from head to the upper thighs (for [^{68}Ga]Ga-FAPI

PET/CT). The following parameters for the CT scan were used: 110 kV, 80 mA, and a slice thickness of 3.75 mm. Acquired data were transferred to the Advantage Workstation (version AW 4.7, GE Healthcare). Image reconstruction was performed using the Bayesian penalized likelihood reconstruction algorithm (Q.clear, GE Healthcare), with a penalization factor (beta) of 500. Routine contrast-enhanced CT (CE-CT) is also performed in all patients as standardized care.

In order to evaluate whether the delayed scan could help differentiate cancerous lesions from inflammation, an additional 3-h [^{68}Ga]Ga-FAPI PET/CT delayed scan (due to ^{68}Ga's relatively short half-life of 68 min) was performed in those who presented increased [^{68}Ga]Ga-FAPI uptake in the whole pancreas and masked the primary tumor. The patients with poor general condition or limited compliance are not required to undergo the delayed scan. The range of the delayed scan includes abdominal and pelvis. The PET/CT acquisition protocol was the same as the 1-h baseline scan, with 2–3 bed positions and 2.5 min/position.

Image analysis and clinical staging

All images were reviewed on the AW 4.7 by two board-certified nuclear medicine physicians (each with > 10 years of experience in PET/CT), who were blinded to the clinical data including CT, MRI, endoscopic ultrasound (EUS), and pathologic results. Any difference in opinion was resolved by consensus. To decrease prejudice, [^{18}F]FDG PET/CT images were interpreted by group 1 (Z.L., S.L.), and [^{68}Ga]Ga-FAPI PET/CT images were interpreted by group 2 (C.H., W.H.). Reviews were performed in the absence of the information from the other PET/CT scan. Image interpretation included semiquantitative and visual interpretations. Contrast-enhanced CT (CE-CT) imaging was interpreted by two board-certified radiologists (W.X, P.Y.) in consensus without knowledge of PET/CT results.

Semiquantitative analysis

For semiquantitative analysis of [^{18}F]FDG and [^{68}Ga]Ga-FAPI PET/CT images, regions of interest (ROIs) were manually delineated on transaxial slices around intense radiopharmaceutical uptake foci. Maximum standard uptake (SUVmax) values were measured automatically through the AW 4.7 workstation. Tracer uptakes for primary tumors, involved lymph nodes, and distant metastases were quantified using SUVmax. The SUVmax of FAPI-avid lesions detected by 1-h baseline scan and by 3-h delayed scan were calculated and compared.

Image interpretation

PET images were analyzed visually. If radiotracer uptake exceeded that of adjacent background tissues, these lesions were coded as positive. The CT findings of PET/CT were used as reference to exclude the possibility of physiological uptake, inflammation, infection, or trauma. Primary pancreatic lesions were classified into three locations: head, body, and tail. Involved lymph nodes were counted independently at four sites: the neck, supraclavicular, mediastinum, abdomen (paraaortic, porta hepatic, retroperitoneal, celiac), and pelvic regions. The brain, lung, liver, and bone were classified as individual metastasis sites. Peritoneum, mesentery, and omentum metastases were uniformly defined as peritoneal carcinomatosis. We calculated the median SUV_{max} and ranges.

On patient-based analysis, we constructed a visual comparative system to intuitively compare the detection capabilities of [^{18}F]FDG and [^{68}Ga]Ga-FAPI PET/CT, based on obviousness (for primary tumors), lesion area (for peritoneal carcinomatosis), or number (for involved lymph nodes and visceral metastases) in the same patient. If the obviousness/area/number of lesions detected by [^{68}Ga]Ga-FAPI PET/CT were superior/larger/more than that of [^{18}F]FDG PET/CT, the result was classified as "FAPI outperformed," and vice versa. If the area or number of lesions detected by the imaging modalities was the same, the result was classified as "equal."

TNM stage was determined according to the 8th edition of the American Joint Committee on Cancer [18]. For patients undergoing initial assessment, we recorded changes in TNM staging based on [^{68}Ga]Ga-FAPI and [^{18}F]FDG PET/CT. Subsequent changes in oncological management were evaluated by two nuclear medicine physicians (CH, WH) and two treating physicians (FL, WS). The referring treating physicians have further been asked what the treatment plan would be prior to and after FAPI PET/CT. All findings and changes were interpreted by consensus.

Statistical analyses

Statistical analyses were performed using SPSS version 22.0 (IBM, Armonk, NY, USA). The Wilcoxon signed-rank tests were used to examine differences between lesion uptake for [^{18}F]FDG and [^{68}Ga]Ga-FAPI and to compare values of baseline and delayed imaging (SUVmax of FAPI PET-positive lesions). Suspected lesions on PET/CT scanning were confirmed through histopathology (following biopsy or surgery) or radiographic follow-up and were used as reference standards. We used McNemar's test to compare differences in detection rates for primary tumors, involved lymph nodes, and metastases. We calculated comparative sensitivity, specificity, and accuracy via McNemar's test to

evaluate the diagnostic efficacy. Statistical significance was set at $P < 0.05$.

Results

Participant characteristics

This retrospective study recruited 36 patients (25/36 men; median age, 60 years; interquartile range, 48–71 years) with suspected or newly diagnosed pancreatic cancer (June 2020–January 2021). Among these patients, 17 were evaluated for discriminating pancreatic mass lesion, and the final diagnosis revealed pancreatic malignancy ($n = 7$, including adenocarcinoma [$n = 3$], adenosquamous carcinoma [$n = 1$], and neuroendocrine tumor [$n = 3$]), a solid pseudopapillary tumor ($n = 1$), pancreatitis ($n = 4$), IgG4-related disease ($n = 2$), a cystadenoma ($n = 1$), and other undefined benign lesions ($n = 2$; the possibility of malignancy was excluded due to no elevated tumor markers, no progression on follow-up imaging, and no evidence of malignancy in the EUS-guided biopsy); 19 patients were evaluated for initial tumor staging, and the final diagnosis revealed adenocarcinoma ($n = 18$, including one with signet-ring cell features) and an acinar cell carcinoma ($n = 1$). Among 26 patients with pancreatic malignancy, 8 underwent surgical resection, including Whipple procedure ($n = 5$), distal pancreatectomy ($n = 2$), and pancreatectomy plus cytoreductive surgery ($n = 1$). The median time interval between the two scans was 2 days (range, 1–6 days). Participant characteristics are presented in Table 1. The radiographic follow-up data was presented in Supplemental material.

Adverse events

All participants tolerated the [^{68}Ga]Ga-FAPI PET/CT scan. No [^{68}Ga]Ga-FAPI-related pharmacological effects or physiological responses occurred. None of the participants reported any abnormal symptoms.

Image interpretation and semiquantitative analysis

In contrast to [^{18}F]FDG, no brain tissue uptake was observed on [^{68}Ga]Ga-FAPI PET/CT, which also showed lower background activity in the liver, heart, and gastrointestinal tract. [^{68}Ga]Ga-FAPI PET/CT had a favorable image contrast with low background activity throughout the body (Fig. 1). In the semiquantitative parameter analysis, [^{68}Ga]Ga-FAPI PET/CT showed higher radiotracer uptake in primary lesions (SUVmax, 21.4 vs. 4.8; $P < 0.001$), involved lymph nodes (SUVmax, 8.6 vs. 2.7; $P < 0.001$), liver metastases (SUVmax, 7.4 vs. 3.7; $P < 0.001$), peritoneal carcinomatosis (SUVmax, 8.4 vs. 2.8; $P < 0.001$), and bone metastases (SUVmax, 10.6 vs. 2.3; $P = 0.001$) (Table 2).

A visual comparative system was established to compare the detection capabilities of [^{18}F]FDG and [^{68}Ga]Ga-FAPI PET/CT. On patient-based comparison, [^{68}Ga]Ga-FAPI PET/CT demonstrated a higher detection capability than [^{18}F]FDG for primary tumor, lymph node, bone, and visceral metastases (Figs. 2 and 3). For visualizing the primary tumor, [^{68}Ga]Ga-FAPI PET/CT was superior to [^{18}F]FDG in 27% (7/26) of patients (Fig. 1, patient nos. 13, 15, 16, 17, 34, tumors indicated by solid arrows). For detecting lymph node, bone, and visceral metastases, [^{68}Ga]Ga-FAPI PET/CT revealed a larger disease extent of peritoneal carcinomatosis in 80% (8/10) of patients (Fig. 1, patient nos. 12, 13, 14, 15, 16, 29, 34; Fig. 4), more liver metastases in 92% (11/12) of patients (Fig. 1, patient nos. 13, 14, 15, 16; Fig. 5), more bone metastases in 83% (5/6) of patients (Fig. 1, patient nos. 13, 15, 29, lesions indicated by dotted arrows), and more abdominal lymph node metastases in 79% (11/14) of patients (Fig. 1, patient nos. 13, 14, 15, 17). Supraclavicular lymph node and pleural metastases (uncommon sites of metastases) were detected by [^{68}Ga]Ga-FAPI PET/CT in two patients (Fig. 1, patient nos. 14, 17); however, these lesions were not visualized using [^{18}F]FDG-PET/CT.

Diagnostic performance

Histopathology or radiographic follow-up were used as references for the diagnostic performance of [^{18}F]FDG and [^{68}Ga]Ga-FAPI PET/CT. All pancreatic mass lesions ($n = 36$) were confirmed via biopsy ($n = 25$), laparoscopic biopsy ($n = 3$), and/or surgical resection ($n = 8$). The final diagnosis revealed 26 patients with pancreatic malignancy. All 26 lesions showed intense uptake of [^{68} Ga]Ga-FAPI; 19/26 lesions showed positive uptake of [^{18}F]FDG. Of the ten patients who were diagnosed with non-malignant disease, seven showed increased [^{68}Ga]Ga-FAPI uptake in the pancreatic mass (patient nos. 7, 27 with IgG4-related pancreatitis, patient nos. 20, 22, 23, 35 with pancreatitis, and patient no. 21 with a solid pseudopapillary tumor), whereas only four (patients 7, 27 with IgG4-related pancreatitis, patients 20, 35 with pancreatitis) showed increased [^{18}F]FDG uptake in the mass lesion. Sensitivity, specificity, and accuracy for the diagnosis of primary tumors were 73.1% (19/26), 60.0% (6/10), and 69.4% (25/36) for [^{18}F]FDG PET/CT and 100% (26/26), 30.0% (3/10), and 80.6% (29/36) for [^{68}Ga]Ga-FAPI PET/CT, respectively (Table 3). [^{68}Ga]Ga-FAPI PET/CT had a higher sensitivity than [^{18}F]FDG, and the difference was statistically significant (100% vs. 73.1%, $P = 0.025$). The specificity of [^{68}Ga]Ga-FAPI PET/CT was lower than [^{18}F]FDG PET/CT, but the difference was not statistically significant (30.0% vs. 60.0%, $P = 0.25$).

Table 1 Summary of patient characteristics

No	Sex	Age	CA19-9*	Jaundice	Clinical indication for PET/CT	Pathology diagnosis	Site of primary lesion	Confirmed metastases	Ways of Confirmation
Patient 1	M	55	142.41	Yes	Evaluation of suspicious mass lesion	Adenosquamous carcinoma	Head	None	**Surgery** (Whipple procedure with lymph node dissection)
Patient 2	F	57	3.66	No	Evaluation of suspicious mass lesion	Undefined benign lesions†	Tail	/	Biopsy, laboratory tests, and radiographic follow-up
Patient 3	M	46	24.37	No	Evaluation of suspicious mass lesion	Undefined benign lesions†	Tail	/	Biopsy, laboratory tests, and radiographic follow-up
Patient 4	M	60	73.92	Yes	Initial staging	Adenocarcinoma	Head	None	**Surgery** (Whipple procedure with lymph node dissection)
Patient 5	M	52	> 700	Yes	Initial staging	Adenocarcinoma	Head	LNM, PC	**Surgery** (Whipple procedure with lymph node dissection)
Patient 6	M	58	NA	No	Initial staging	Adenocarcinoma	Body	LM	PT: biopsy LM: radiographic follow-up
Patient 7	M	59	3.79	No	Evaluation of suspicious mass lesion	IgG4-related pancreatitis	Tail	/	Biopsy and laboratory tests
Patient 8	F	84	244.49	Yes	Initial staging	Adenocarcinoma	Head	LNM	PT: biopsy LNM: EUS biopsy and radiographic follow-up
Patient 9	M	69	> 700	No	Initial staging	Adenocarcinoma	Tail	LNM	**Surgery** (distal pancreatectomy with lymph node dissection)
Patient 10	M	65	> 700	No	Initial staging	Adenocarcinoma	Tail	LM, PC	PT: biopsy LM and PC: radiographic follow-up
Patient 11	F	56	30.75	No	Evaluation of suspicious mass lesion	Adenocarcinoma	Head	LNM, LM, PC	PT: biopsy LNM, LM, and PC: radiographic follow-up
Patient 12	F	55	16.12	No	Initial staging	Acinar cell carcinoma	Tail	LNM, PC	**Surgery** (total pancreatectomy plus cytoreductive surgery)
Patient 13	M	61	> 700	Yes	Initial staging	Adenocarcinoma	Body and tail	LNM, LM, PC, BM, PM	PT: biopsy LNM, LM, PC, BM, and PM: radiographic follow-up
Patient 14	F	57	> 700	No	Initial staging	Adenocarcinoma	Tail	LNM, LM, PC, PM	PT: biopsy LM: percutaneous biopsy LNM, PC, and PM: radiographic follow-up
Patient 15	F	62	> 700	No	Initial staging	Adenocarcinoma	Tail	LM, BM	PT: biopsy LM and BM: radiographic follow-up

Table 1 (continued)

No	Sex	Age	CA19-9*	Jaundice	Clinical indication for PET/CT	Pathology diagnosis	Site of primary lesion	Confirmed metastases	Ways of Confirmation
Patient 16	M	85	> 700	No	Initial staging	Adenocarcinoma	Head	LNM, LM	PT: biopsy LM: percutaneous biopsy LNM: radiographic follow-up
Patient 17	F	65	> 700	No	Initial staging	Adenocarcinoma	Body	None	PT: biopsy
Patient 18	M	65	NA	No	Evaluation of suspicious mass lesion	Adenocarcinoma	Body and tail	LNM, PC	PT: biopsy LNM and PC: radiographic follow-up
Patient 19	F	47	20.56	No	Evaluation of suspicious mass lesion	Neuroendocrine tumor, G2 (NET-G2)	Body and tail	LM	PT: **surgery** (distal pancreatectomy) LM: percutaneous biopsy
Patient 20	M	71	37.95	Yes	Evaluation of suspicious mass lesion	Pancreatitis	Body and tail	/	Laparoscopic biopsy and laboratory tests
Patient 21	M	51	26.72	No	Evaluation of suspicious mass lesion	Solid pseudopapillary tumor	Head	/	Biopsy
Patient 22	M	56	10.25	No	Evaluation of suspicious mass lesion	Pancreatitis	Tail	/	Biopsy, laboratory tests, and radiographic follow-up
Patient 23	M	75	432.86	No	Evaluation of suspicious mass lesion	Pancreatitis	Head	/	Biopsy, laboratory tests, and radiographic follow-up
Patient 24	M	56	NA	No	Evaluation of suspicious mass lesion	Cystadenoma	Head	/	Laparoscopic biopsy and radiographic follow-up
Patient 25	M	53	3.43	No	Evaluation of suspicious mass lesion	Neuroendocrine tumor, G3 (NET-G3)	Head	LM	PT: biopsy LM: percutaneous biopsy
Patient 26	M	73	> 700	Yes	Initial staging	Adenocarcinoma	Head	None	**Surgery** (Whipple procedure)
Patient 27	M	71	7.72	No	Evaluation of suspicious mass lesion	IgG4-related pancreatitis	Head	/	Laparoscopic biopsy and laboratory tests
Patient 28	M	68	14.8	No	Initial staging	Adenocarcinoma	Head	LNM	**Surgery** (Whipple procedure with lymph node dissection)
Patient 29	M	53	581.73	No	Initial staging	Adenocarcinoma (with signet ring cell features)	Tail	PC, BM	PT: biopsy PC and BM: percutaneous biopsy
Patient 30	M	79	189.55	Yes	Initial staging	Adenocarcinoma	Head	None	Biopsy
Patient 31	M	73	501.68	Yes	Initial staging	Adenocarcinoma	Head	None	Biopsy
Patient 32	F	61	> 700	No	Evaluation of suspicious mass lesion	Adenocarcinoma	Head	LM	PT: biopsy LM: percutaneous biopsy
Patient 33	M	48	3.59	Yes	Initial staging	Adenocarcinoma	Head	LM	PT: biopsy LM: percutaneous biopsy
Patient 34	F	60	> 700	No	Initial staging	Adenocarcinoma	Body and tail	PC	PT: biopsy PC: percutaneous biopsy

Table 1 (continued)

No	Sex	Age	CA19-9*	Jaundice	Clinical indication for PET/CT	Pathology diagnosis	Site of primary lesion	Confirmed metastases	Ways of Confirmation
Patient 35	M	67	213.28	No	Evaluation of suspicious mass lesion	Pancreatitis	Tail	/	Biopsy, laboratory tests, and radiographic follow-up
Patient 36	F	51	55.65	Yes	Evaluation of suspicious mass lesion	Neuroendocrine tumor, G3 (NET-G3)	Head	None	PT: biopsy

*CA19-9 normal range: 0–37 U/mL. Abbreviations: *PT* primary tumor, *LNM* lymph node metastases, *LM* liver metastases, *PC* peritoneal carcinomatosis, *PM* pleural metastases, *BM* bone metastases

†The possibility of malignancy was excluded through endoscopic ultrasound (EUS) biopsy, a lack of elevated tumor markers, and no progression on follow-up imaging

The radiographic follow-up data was presented in Supplemental material

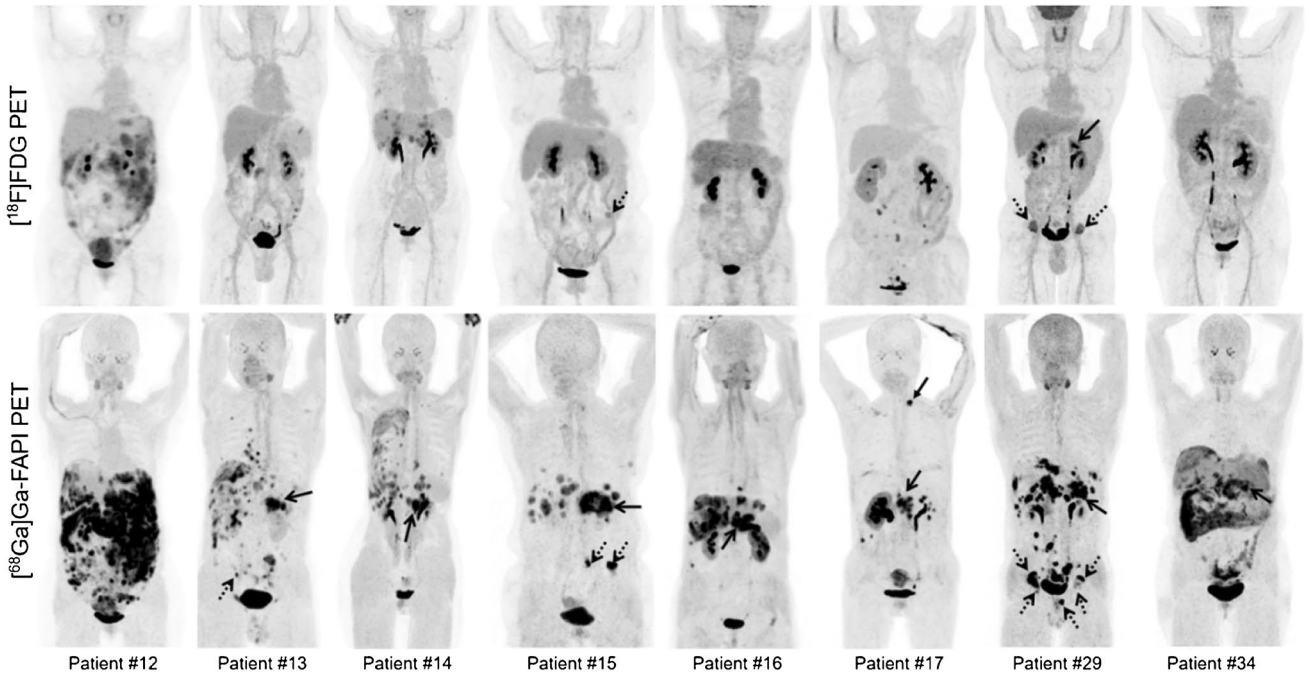

Fig. 1 Eight representative patients with pancreatic cancer underwent [^{18}F]-fluorodeoxyglucose ([^{18}F]FDG) and [^{68}Ga]Ga-labeled fibroblast activation protein inhibitor ([^{68}Ga]Ga-FAPI) positron emission tomography/computed tomography (PET/CT) imaging. [^{68}Ga]Ga-FAPI PET/CT outperformed [^{18}F]FDG PET/CT in detecting primary tumors (patient nos.13, 14, 15, 16, 17, 29, 34; indicated with solid arrows), supraclavicular lymph node metastases (patient no. 17, indicated with arrowhead), abdomen lymph node metastases (patient nos. 13, 14, 15, 17), liver metastases (patient nos. 13, 14, 15, 16), peritoneal carcinomatosis (patient nos. 12, 13, 14, 15, 16, 29, 34), pleural metastases (patient nos.13, 14), and bone metastases (patient nos.13, 15, 29; indicated with dotted arrows)

A total of 169 lymph nodes were identified in 17 patients and confirmed via lymph node dissection ($n=129$), biopsy ($n=2$), or radiographic follow-up ($n=38$). Of these, 22 lymph nodes (in 10 patients) were positive for malignancy. Lymph node involvement included 13 true-positive, 28 false-positive, nine false-negative, and 119 true-negative findings on [^{18}F]FDG PET/CT and 18 true-positive, 21 false-positive, four false-negative, and 126 true-negative findings on [^{68}Ga]Ga-FAPI PET/CT. In the node-based analysis, the sensitivity, specificity, and accuracy of [^{18}F]FDG PET/CT were 59.1%, 81.0%, and 78.1%, respectively, and the sensitivity, specificity, and accuracy of [^{68}Ga]Ga-FAPI PET/CT were 81.8%, 85.7%, and 85.2%, respectively (Table 3). Although sensitivity and specificity were not statistically significantly different between [^{68}Ga]Ga-FAPI and [^{18}F]FDG, [^{68}Ga]Ga-FAPI surpassed [^{18}F]FDG in terms of sensitivity (81.8 vs. 59.1%, $P=0.063$) and specificity (85.7 vs. 81.0%, $P=0.065$) of the involved lymph nodes.

Table 2 Comparison of [^{18}F]FDG and [^{68}Ga]Ga-FAPI uptake in primary and metastatic lesions in pancreatic cancer

Parameters	No. of patients	Lesions size (cm)		[^{18}F]FDG uptake			[^{68}Ga]Ga-FAPI uptake			*P* value (SUV-FDG vs. SUV-FAPI)
		Median	Range	Median SUVmax	Range of SUVmax	No. of positive lesions	Median SUVmax	Range of SUVmax	No. of positive lesions	
Malignant tumors*	26	3.9	2.2–8.0	4.8	2.3–10.9	19	21.4	11.6–34.9	26	< 0.001
Involved lymph nodes										
Neck†	1	1.1	NA	2.4	NA	0	13.3	NA	1	NA
Mediastinum	1	0.7	NA	1.0	NA	0	10.8	NA	1	NA
Abdomen‡	14	0.9	0.5–2.1	2.8	1.4–6.8	23	8.2	2.9–18.4	43	< 0.001
All	15	0.9	0.5–2.1	2.7	1.0–6.8	23	8.6	2.9–18.4	45	< 0.001
Bone and visceral metastases										
Liver	12	1.4	0.8–6.9	3.7	2.6–6.4	15	7.4	3.9–13.0	74	< 0.001
Peritoneal	10	1.6	0.5–14.1	2.8	1.2–9.3	33	8.4	1.5–35.4	77	< 0.001
Bone	6	1.3	0.6–3.1	2.3	1.1–8.5	7	10.6	3.9–33.8	14	0.001
Pleural§	2	1.0	0.7–1.3	2.4	1.3–3.6	NA	6.9	5.5–9.5	NA	NA
All	17	1.4	0.5–14.1	3.5	1.1–9.3	55	7.9	1.5–35.4	165	< 0.001

*Malignant tumors include one adenosquamous carcinoma, three neuroendocrine tumors, one acinar cell carcinoma, and 21 adenocarcinomas

†Lymph nodes in neck regions include neck and supraclavicular lymph nodes

‡Lymph nodes in abdominal regions include porta hepatic, retroperitoneal, and celiac lymph nodes

§In two patients with widespread pleural metastases, the number of positive lesions could not be counted (lesions too numerous to count)

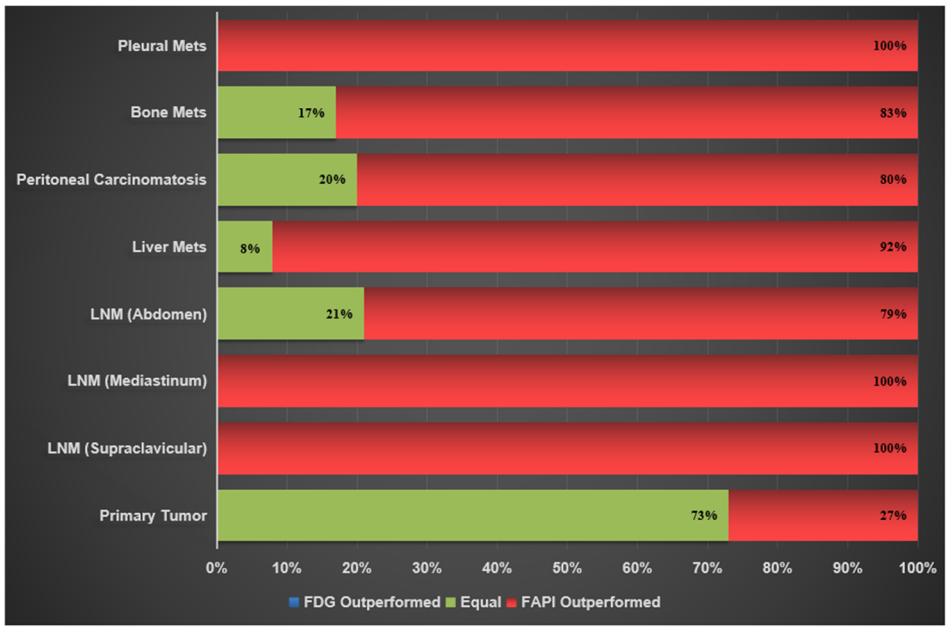

Fig. 2 A visual comparative system was constructed to compare the detection capabilities of [^{18}F]fluorodeoxyglucose ([^{18}F]FDG) and [^{68}Ga]Ga-labeled fibroblast activation protein inhibitor ([^{68}Ga]Ga-FAPI) positron emission tomography/computed tomography (PET/CT) for primary tumors, involved lymph nodes, and distant metastases. Note: LNM lymph nodes metastases, Liver Mets liver metastases, Pleural Mets pleural metastases, Bone Mets bone metastases

Parameters	Primary Tumor	LNM (Supraclavicular)	LNM (Mediastinum)	LNM (Abdomen)	Liver Mets	Peritoneal Carcinomatosis	Bone Mets	Pleural Mets
FAPI Outperformed	7	1	1	11	11	8	5	2
Equal	19	0	0	3	1	2	1	0
FDG Outperformed	0	0	0	0	0	0	0	0

Regarding diagnostic performance for bone and visceral metastases, we evaluated 164 suspicious lesions in 16 patients. Pathologic data via surgery ($n=61$), biopsy ($n=43$), or radiographic follow-up ($n=60$) were used to evaluate suspicious lesions. Of these, 141 lesions (in 16 patients) were confirmed as tumor metastases. In the lesion-based analysis, sensitivity, specificity, and accuracy in the diagnosis of bone and visceral metastases were 44.0% (62/141), 73.9% (17/23), and 48.2% (79/164), respectively, on [^{18}F]FDG PET/CT, compared with 91.5% (129/141), 65.2% (15/23), and 87.8% (144/164), respectively, on [^{68}Ga]Ga-FAPI PET/CT (Table 3). Thus, the sensitivity and accuracy of [^{68}Ga]Ga-FAPI were superior to those of [^{18}F]FDG ($P<0.001$ and $P<0.001$, respectively). The specificity of [^{68}Ga]Ga-FAPI was similar to that of [^{18}F]FDG ($P=0.50$).

TNM staging and clinical management

Among 23 patients with pancreatic cancer, [^{68}Ga]Ga-FAPI PET/CT upgraded the N stage in 7 patients (7/23, 30.4%) and the M stage in 5 patients (5/23, 21.7%) compared with [^{18}F]FDG PET/CT (Table 4). [^{68}Ga]Ga-FAPI PET/CT demonstrated a greater number of involved lymph nodes in patient nos. 9, 11, 13, 14, 16, 17, and 18. Unexpected distant metastases detected by [^{68}Ga]Ga-FAPI PET/CT were located in the liver (patient nos. 6, 10, 13, 15, 16, 26), peritoneum (patient nos. 10, 13, 34), and bones (patient nos. 6, 11, 13). With the new lesions detected via [^{68}Ga]Ga-FAPI PET/CT, TNM staging was eventually upstaged in 6 patients (6/23, 26.1%): one from IIA to IIB, one from IIA to IV, three from IIB to IV, and one from III to IV. Consequently, the therapeutic regimen was changed in 2 patients (2/23, 8.7%; from surgically resectable to unresectable) due to newly detected liver/bone metastases and peritoneal carcinomatosis (Table 4).

Compared with CE-CT, [^{68}Ga]Ga-FAPI PET/CT upgraded the N stage in 6 patients (6/23, 26.1%) and the M stage in 4 patients (4/23, 17.4%). However, [^{68}Ga]Ga-FAPI PET/CT also underestimated the T stage in one patient (due to the vascular involvement detected by CE-CT). As a result, TNM staging was finally upstaged in 5 patients (5/23, 21.7%), and therapeutic regimen was changed in only one patient (1/23, 4.3%).

Based on these findings, [^{68}Ga]Ga-FAPI PET/CT did not obviously modify the probability of management change when compared with contrast-enhanced CT and ^{18}F-FDG PET/CT. The comparative results for TNM staging with CE-CT, [^{18}F]FDG PET/CT, and [^{68}Ga]Ga-FAPI PET/CT are summarized in Table 4.

[^{68}Ga]Ga-FAPI uptake in tumor-associated pancreatitis and cholangitis

Intense [^{68}Ga]Ga-FAPI uptake was observed throughout the pancreas in 12/26 patients with pancreatic malignancy. It was not possible to distinguish between pancreatic tumors

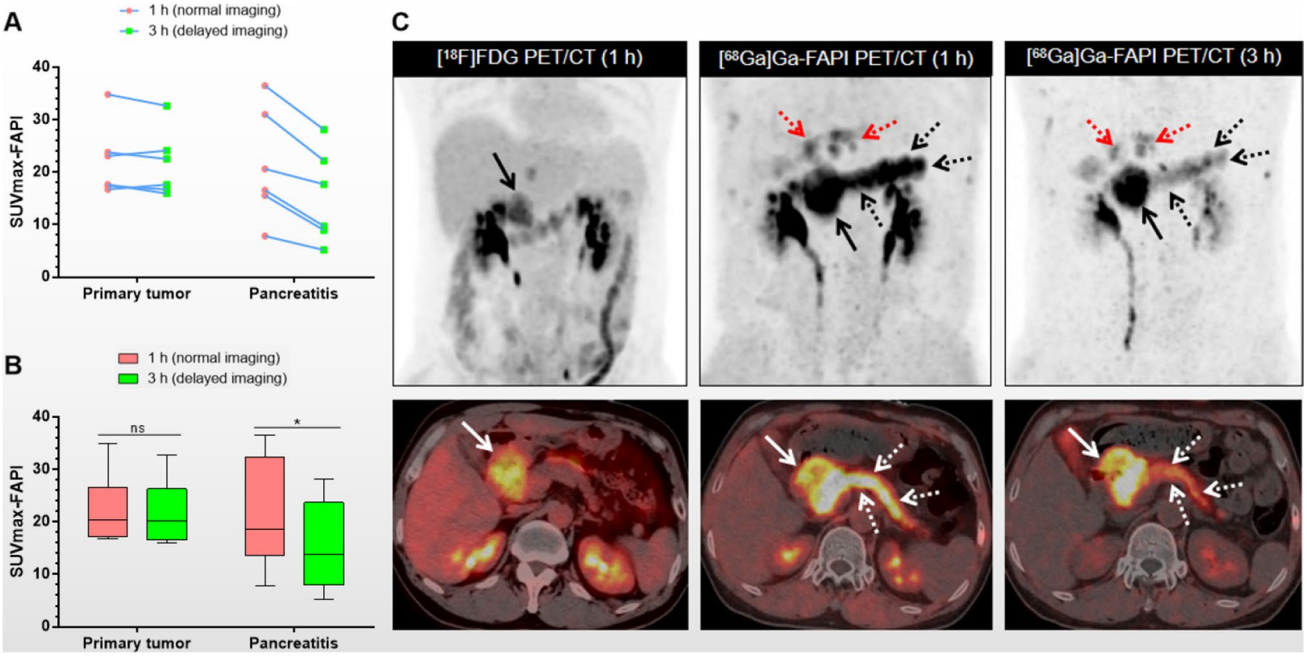

Fig. 3 [^{68}Ga]Ga-labeled fibroblast activation protein inhibitor ([^{68}Ga]Ga-FAPI) uptake assessment of six patients with pancreatic cancer and pancreatitis in a 1-h normal image and a 3-h delayed image. The trend of maximum standard uptake values (SUVmax) of tumor and pancreatitis lesions visualized with FAPI in a 1-h normal image and a 3-h delayed image are shown in **A**. **B** The median and range of SUVmax-FAPI for the tumor and pancreatitis in a 1-h normal image and a 3-h delayed image. The representative patient was a 48-year-old man with pancreatic cancer visible on the [^{18}F]-fluorodeoxyglucose ([^{18}F]FDG) positron emission and computed tomography (PET/CT) scan (**C**, left line), and the metabolic activity of the primary tumor was high (SUVmax: 9.4, indicated with a solid arrow). However, the 1-h image for [^{68}Ga]Ga-FAPI PET/CT (**C**, middle line) demonstrated intense [^{68}Ga]Ga-FAPI uptake in the primary tumor (SUVmax: 16.8, solid arrow), the intrahepatic bile duct (red dotted arrows), and the body and tail of the pancreas (SUVmax: 15.6, white and black dotted arrows). To differentiate between malignant and benign lesions, 3-h delayed imaging of [^{68}Ga]Ga-FAPI PET/CT was performed (**C**, right line). The SUVmax value of the primary tumor was slightly elevated (SUVmax: 17.6, solid arrow), and the SUVmax values of the pancreatitis lesions were decreased (SUVmax: 9.0, white and black dotted arrow) compared to the 1-h [^{68}Ga]Ga-FAPI PET/CT images

and pancreatitis in 8/12 patients based on the semiquantitative analysis due to similar [^{68}Ga]Ga-FAPI uptake rates (SUVmax-tumor vs. SUVmax-pancreatitis: 26.4 vs. 22.0, $P = 0.069$). Among these patients, only one had been diagnosed with chronic pancreatitis before [^{68}Ga]Ga-FAPI PET/CT. We speculated that the increased [^{68}Ga]Ga-FAPI uptake in the majority of these patients was due to tumor-associated pancreatitis; 4/12 patients subsequently underwent radical pancreatectomy after [^{68}Ga]Ga-FAPI PET/CT, and postoperative pathology confirmed the diagnosis of pancreatic cancer and pancreatitis.

Since neither visual interpretation nor semiquantitative analysis could distinguish pancreatitis from pancreatic cancer on the 1-h [^{68}Ga]Ga-FAPI, we further explored whether the delayed PET/CT scan could play a role. An additional delayed [^{68}Ga]Ga-FAPI scan (3 h after tracer injection) was performed in six patients with both pancreatic cancer and pancreatitis. The other 6 patients did not undergo the delayed scan due to the poor general status or limited compliance. Results indicated that stable [^{68}Ga]Ga-FAPI uptake in pancreatic tumors were observed between the 1-h and 3-h scans (median SUVmax, 20.4 vs. 20.1; $P = 0.249$); we observed decreased [^{68}Ga]Ga-FAPI uptake within pancreatitis (median SUVmax, 18.6 vs. 13.7; $P = 0.028$) (Fig. 3A–B). Representative images from early and delayed scans are shown in Fig. 3C.

Increased [^{68}Ga]Ga-FAPI uptake was observed in the intrahepatic bile ducts and common bile duct in ten of the 36 patients. However, increased activity was not observed in the corresponding [^{18}F]FDG PET/CT. Among the 10 patients, nine were diagnosed with pancreatic cancer, and one had IgG4-related pancreatitis. Dilation of the intrahepatic bile ducts and the common bile duct was observed in all ten patients, and jaundice was observed in eight patients. Increased [^{68}Ga]Ga-FAPI uptake was mainly caused by tumor-induced obstructive cholangitis. Similar to pancreatitis, we observed the decreased [^{68}Ga]Ga-FAPI uptake within the hepatobiliary tract in four of the six patients who underwent dual-time point PET scan (median SUVmax of cholangitis: 11.7 vs. 8.0) (Fig. 3C), but the difference was not statistically significant ($P = 0.068$).

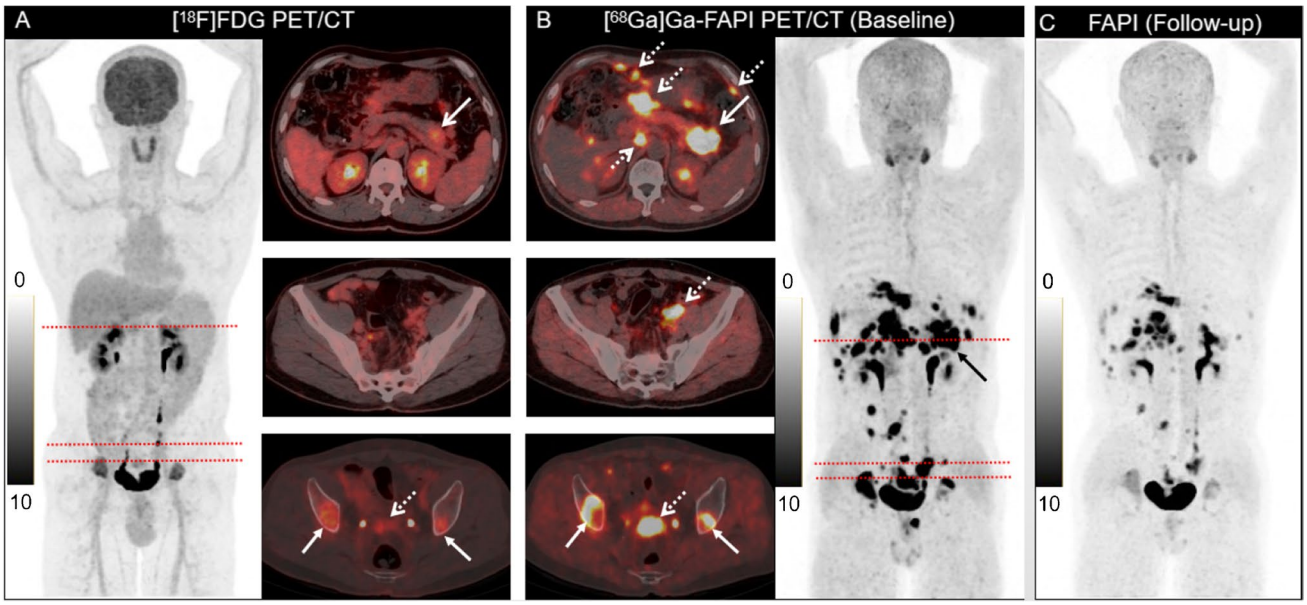

Fig. 4 A representative patient with additional findings for the primary pancreatic tumor and peritoneal and bone metastases. The patient was a 53-year-old man with known pancreatic ductal adenocarcinoma (with signet-ring cell features) who underwent PET/CT. [^{18}F]-fluorodeoxyglucose ([^{18}F]FDG) PET/CT showed moderate [^{18}F]FDG uptake in the primary tumor, with a SUVmax of 5.8 (indicated with a solid arrow) and several bone metastases (arrowheads). Although multiple nodules of the omentum, peritoneum, and mesentery were revealed via [^{18}F]FDG PET/CT, these lesions had low-to-moderate metabolic activity (dotted arrow) (**A**). In [^{68}Ga]Ga-labeled fibroblast activation protein inhibitor ([^{68}Ga]Ga-FAPI) PET/CT imaging, higher radiotracer uptake was observed on the primary lesion (SUVmax 30.4, solid arrow), bone metastases (arrowheads), and peritoneal carcinomatosis (dotted arrows). In addition, [^{68}Ga]Ga-FAPI PET/CT demonstrated the involved location and scope of peritoneal carcinomatosis more effectively than [^{18}F]FDG (**B**). Follow-up [^{68}Ga]Ga-FAPI PET/CT after three cycles of chemotherapy reveals a partial response (measurable target lesions, 38% decrease in the sum of the longest diameters) (**C**)

Discussion

Though surgical resection is the only potentially curative therapy for pancreatic cancer, pancreatic cancer is difficult to accurately diagnose at resectable stages [2]. Conventional [^{18}F]FDG PET/CT is of limited use for tumor staging and surgical planning in pancreatic cancer. Therefore, the development of novel PET tracers is of great significance to improve the diagnostic performance of PET/CT. In the present study, we evaluated the clinical utility of PET/CT with [^{68}Ga]Ga-FAPI (a PET tracer used for visualization of tumor stroma) for the diagnosis of primary and metastatic lesions in patients with pancreatic malignancies, and in comparison with [^{18}F]FDG PET/CT. Our results indicated that [^{68}Ga]Ga-FAPI PET/CT was superior to [^{18}F]FDG in detecting primary and metastatic lesions. Compared with the [^{18}F]FDG-based TNM stage, the [^{68}Ga]Ga-FAPI-based TNM stage was upgraded in 6 patients (6/23, 26.1%), resulting in management changes in 2 patients (2/23, 8.7%). However, the therapeutic regimen was changed in only one patient when compared with CE-CT (1/23, 4.3%). As such, the standard of care imaging which included a [^{68}Ga]Ga-FAPI PET/CT did not significantly modify the clinical management in this study.

Regarding the assessment of primary tumors, [^{18}F]FDG PET/CT has unsatisfactory sensitivity in the detection of pancreatic cancer, especially small tumors (< 20 mm). In this study, [^{68}Ga]Ga-FAPI PET/CT had a higher sensitivity than [^{18}F]FDG PET/CT for detecting pancreatic cancer. This finding will help improve physician's diagnostic confidence and reduce the proportion of missed diagnosis. It is known that pancreatic tumors are characterized by intense stromal desmoplastic reactions surrounding cancer cells, and CAFs are the main effector cells in the desmoplastic reaction. Therefore, intense uptake of [^{68}Ga]Ga-FAPI was observed in pancreatic cancer, resulting in a favorable target-to-background ratio (TBR) and clear tumor boundary from [^{68}Ga]Ga-FAPI PET/CT. A clear tumor boundary could improve the delineation of the gross tumor volume for radiotherapy planning [19]. This implies that [^{68}Ga]Ga-FAPI PET/CT may hold clinical utility in the early diagnosis of pancreatic cancer and may provide additional information for target volume delineation.

Previous studies have reported that [^{68}Ga]Ga-FAPI was not a more tumor-specific tracer than [^{18}F]FDG and [^{68}Ga]Ga-FAPI also accumulates in many non-oncological conditions [20–23]. In this study, different factors may account for the increased [^{68}Ga]Ga-FAPI in the benign pancreatic mass.

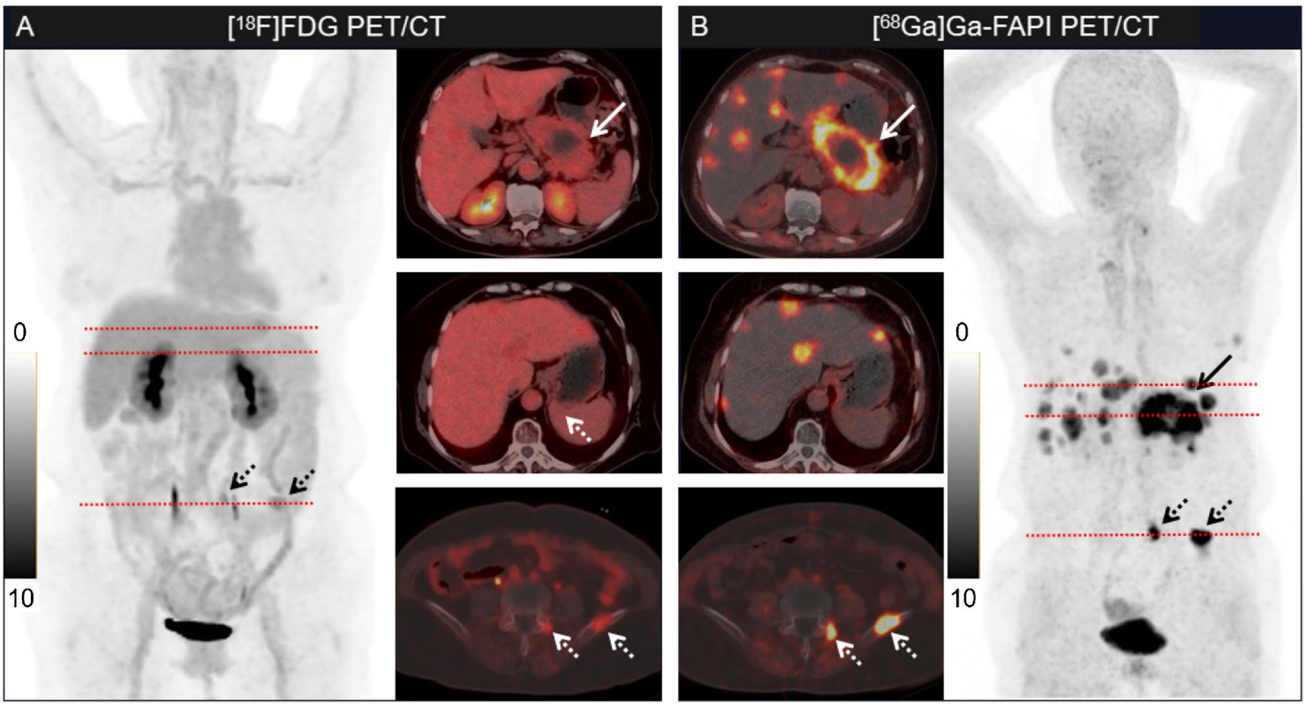

Fig. 5 A representative patient with additional findings for the primary pancreatic tumor and liver metastases. A 62-year-old woman with known pancreatic ductal adenocarcinoma underwent [^{18}F]-fluorodeoxyglucose ([^{18}F]FDG) PET/CT for initial staging before therapy. [^{18}F]FDG PET/CT showed low-to-moderate [^{18}F]FDG uptake (with a SUVmax of 4.0) in the primary tumor of the pancreatic body and tail (indicated with a solid arrow); moderate metabolic activity was observed in the lytic bone destruction lesions (dotted arrow) (**A**). [^{68}Ga]Ga-FAPI PET/CT demonstrated higher radiotracer uptake in both the primary tumor (SUVmax 16.2, solid arrow) and bone metastases (dotted arrows) compared with [^{18}F]-FDG PET/CT. A greater number of liver metastases were observed in the [^{68}Ga]Ga-FAPI PET/CT; most of these lesions were negative in the [^{18}F]FDG PET/CT (**B**)

Table 3 Diagnostic performances of [^{18}F]FDG and [^{68}Ga]Ga-FAPI PET/CT in assessment of primary and metastatic lesions (lesion-based analysis)

Parameters	[^{18}F]FDG PET/CT			[^{68}Ga]Ga-FAPI PET/CT		
	Sensitivity (%)	Specificity (%)	Accuracy (%)	Sensitivity (%)	Specificity (%)	Accuracy (%)
Primary tumor	73.1% (19/26) [57, 85]	60.0% (6/10) [35, 81]	69.4% (25/36) [56, 80]	100.0% (26/26) [89, 100]	30.0% (3/10) [12, 56]	80.6% (29/36) [64, 91]
Lymph node metastases	59.1% (13/22) [39, 77]	81.0% (119/147) [74, 87]	78.1% (132/169) [71, 84]	81.8% (18/22) [61, 93]	85.7% (126/147) [79, 91]	85.2% (144/169) [79, 90]
Bone and visceral metastases	44.0% (62/141) [36, 52]	73.9% (17/23) [53, 88]	48.2% (79/164) [41, 56]	91.5% (129/141) [86, 95]	65.2% (15/23) [45, 81]	87.8% (144/164) [82, 92]

Numbers in parentheses are the numbers of lesions used to calculate the percentage

Numbers in brackets are 95% CIs

Intense [^{68}Ga]Ga-FAPI uptake was observed in patients with pancreatitis (patient 20, 22, 23 and 35); this is because [^{68}Ga]Ga-FAPI had an affinity for inflammatory cells, which may also activate fibrotic reaction and manifest avidity for [^{68}Ga]Ga-FAPI [24]. High accumulation of [^{68}Ga]Ga-FAPI was also noted in IgG4-related disease (patients 7 and 27), which is histopathologically characterized by storiform fibrosis [25]. To be more specific, myofibroblasts and fibroblasts are activated by polarized CD4-positive T-cell population to drive the fibrotic process in IgG4-related disease [26]. Therefore, we speculate that the increased [^{68}Ga]Ga-FAPI uptake in IgG4-related disease results from the uptake by the activated fibroblasts or myofibroblasts. Due to the increased [^{68}Ga]Ga-FAPI uptake in these non-oncological diseases, [^{68}Ga]Ga-FAPI PET/CT had lower specificity for the diagnosis of pancreatic mass lesion than that of [^{18}F]FDG PET/

Table 4 Comparison of CE-CT, [^{18}F]FDG, and [^{68}Ga]Ga-FAPI PET/CT-based TNM staging of 23 treatment-naive patients with pancreatic cancer

No	TNM stage (CE-CT-based)	TNM stage (FDG-based)	TNM stage (FAPI-based)	Additional finding on FAPI PET/CT (compared to CE-CT)	Staging change (compared to CE-CT)	Additional finding on FAPI PET/CT (compared to FDG)	Staging change (compared to FDG)
Patient 1	T2N0Mx	T2N0M0	T2N0M0	None	None	None	None
Patient 4	T2N0Mx	T2N0M0	T2N0M0	None	None	None	None
Patient 5	T2N0Mx	T2N0M0	T2N0M0	None	None	None	None
Patient 6	T3N1M1	T3N1M0	T3N1**M1**	Bone mets, greater number of liver mets	None	Bone and liver mets	**Upstaged**
Patient 8	T2N2Mx	T2N2M0	T2N2M0	None	None	None	None
Patient 9	T3N0Mx	T3N0M0	T3**N1**M0	Abdominal LN mets	**Upstaged**	Abdominal LN mets	**Upstaged**
Patient 10	T2N2M1	T2N2M0	T2N2**M1**	PC, greater number of liver mets	None	PC, liver mets	**Upstaged**
Patient 11	T4N1Mx	T4N1M1	T4**N2**M1	More abdominal LN mets; liver and bone mets, PC	**Upstaged**	More abdominal LN, liver, and bone mets; larger disease extent of PC	None
Patient 12	T4N1M1	T4N1M1	T4N1M1	Larger disease extent of PC	None	None	None
Patient 13	T3N2M1	T3N1M0	T3**N2M1**	Greater number of liver, bone, and pleural mets; larger disease extent of PC	None	Greater number of abdominal LN mets; liver, bone, and pleural mets; PC	**Upstaged**
Patient 14	T2N0M1	T2N0M1	T2**N1**M1	Abdominal LN and pleural mets, greater number of liver mets, PC	None	Abdominal LN and pleural mets, greater number of liver mets, larger disease extent of PC	None
Patient 15	T4N0M1	T4N0M1	T4N0M1	Greater number of liver mets; bone mets, PC	None	Greater number of liver mets; bone mets	None
Patient 16	T3N0M1	T3N0M0	T3**N1M1**	Mediastinal LN mets; greater number of liver mets	None	Mediastinal LN and liver mets	**Upstaged**
Patient 17	T3N1M0	T3**N0**M1	T3**N2M1**	Supraclavicular and abdominal LN mets; PC	**Upstaged**	Supraclavicular and abdominal LN mets; larger disease extent of PC	None
Patient 18	T2N1M1	T2N1M1	T2**N2**M1	Abdominal LN mets; larger disease extent of PC	None	Abdominal LN mets; larger disease extent of PC	None
Patient 26	T2N1M0	T2N1M0	T2N1**M1**	Liver mets	**Upstaged**	Liver mets	**Upstaged**
Patient 28	T2N2Mx	T2N2M0	T2N2M0	None	None	None	None
Patient 29	T2N1Mx	T2N1M1	T2N1M1	Bone mets, PC	**Upstaged**	Larger disease extent of PC	None
Patient 30	T3N0Mx	T3N0M0	T3N0M0	None	None	None	None
Patient 31	T4N0Mx	T4N0M0	T4N0M0	None	None	None	None
Patient 32	T3N1M1	T3N1M1	T3N1M1	Greater number of liver mets	None	Greater number of liver mets	None
Patient 33	T4N0M1	T3N0M1	T3N0M1	Greater number of liver mets	None	Greater number of liver mets	None
Patient 34	T4N0M1	T4N0M1	T4N0M1	Larger disease extent of PC	None	Larger disease extent of PC	None

Abbreviations: Mets metastases, *PC* peritoneal carcinomatosis, *LN* lymph node

CT. Considering sometimes the pancreatitis occurred along with malignant disease, image interpretation must take into consideration of other imaging findings (including contrast-enhanced CT and MR) and clinical data rather than solely based on the uptake level of [^{68}Ga]Ga-FAPI.

Lymph node metastasis is the main metastatic pattern of pancreatic cancer, typically occurring in the early phase [27]. The number of involved lymph nodes and the lymph node ratio (LNR) are closely associated with pancreatic cancer prognosis [28]. Thus, accurate assessment of lymph node metastasis is important, and [^{18}F]FDG PET/CT has low-to-moderate sensitivity in the evaluation of lymph node metastasis [5, 29]. In our study, [^{68}Ga]Ga-FAPI PET/CT demonstrated a greater number of involved lymph nodes than [^{18}F]FDG PET/CT, resulting in high sensitivity. The N stage was upstaged in seven patients (7/26, 26.9%) using [^{68}Ga]Ga-FAPI PET/CT, which benefits from higher radiotracer uptake and lower physiological uptake. Thus, [^{68}Ga]Ga-FAPI PET/CT may overcome existing problems in the accurate assessment of N staging and better rationalize surgical planning and may thereby improve the prognosis of pancreatic cancer.

Liver metastasis is one of the most common distant metastatic modes in pancreatic cancer and strongly influences prognosis. In patients with hepatic oligometastasis, synchronous resection of primary tumors and liver metastases prolongs patients' median overall survival (14.5–16.8 months) [30]. [^{18}F]FDG PET/CT has some limitations in detecting liver metastases, including high physiological metabolic uptake in the liver and poor visualization of small metastases [31, 32]. This study demonstrated that [^{68}Ga]Ga-FAPI PET/CT outperformed [^{18}F]FDG PET/CT in detecting liver metastasis. There is no physiological uptake of [^{68}Ga]Ga-FAPI in the normal liver, leading to a high target-to-background ratio for [^{68}Ga]Ga-FAPI PET/CT. In this study, [^{68}Ga]Ga-FAPI PET/CT detected liver metastases in six patients (identifying liver metastases as small as 0.78 cm), whereas [^{18}F]FDG PET/CT missed all lesions. Accurate diagnosis of liver metastases with [^{68}Ga]Ga-FAPI PET/CT could help guide oncologic management, especially for patients with hepatic oligometastasis (patient nos. 10, 11, and 25 in this study).

Peritoneal carcinomatosis is another common distant metastatic pattern in pancreatic cancer; accurate assessment is crucial for selecting an appropriate therapy regimen [33]. Previous studies demonstrated the superiority of [^{68}Ga]Ga-FAPI PET/CT for detecting peritoneal carcinomatosis in various types of cancer [34]; the present study confirmed the usefulness of [^{68}Ga]Ga-FAPI PET/CT in the evaluation of peritoneal carcinomatosis in pancreatic cancer. This result may be explained by the strong fibrotic response when tumors invade peritoneal tissue (increased tumor uptake) and no interference of physiological uptake within the gastrointestinal tract (low background uptake).

Increased [^{68}Ga]Ga-FAPI uptake was observed in patients with tumor-associated pancreatitis and cholangitis. Intense [^{68}Ga]Ga-FAPI uptake (especially in pancreatitis) in inflammation may mask tumor activity in pancreatic cancer [13, 24]. In previous oncological imaging studies [35–37], the additional delayed scan has been considered to offer substantial advantage for the discrimination of cancerous lesion versus non-cancerous lesions, as the malignant tumor usually show a further increase in tracer accumulation on the late scans. Benign lesions, on the other hand, usually show a decrease in SUVs. Therefore, we conducted an additional 3-h delayed [^{68}Ga]Ga-FAPI PET/CT scan to discriminate pancreatic cancer from pancreatitis in 6 patients. The results demonstrated that the dual-time imaging in all 6 patients indicated differential uptake kinetics in pancreatic cancer (stable [^{68}Ga]Ga-FAPI uptake) and tumor-associated pancreatitis (decreased [^{68}Ga]Ga-FAPI uptake). A similar phenomenon was observed in tumor-induced cholangitis in three patients. These findings are similar to those of a recent study [16]. Therefore, the different uptake kinetics of [^{68}Ga]Ga-FAPI might help differentiate pancreatic cancer from pancreatitis. Studies with larger patient cohorts are needed to confirm this finding.

In this study, [^{68}Ga]Ga-FAPI PET/CT revealed more metastatic lesions than [^{18}F]FDG PET/CT and led to upstaging of TNM stage, especially in identifying abdominal lymph node, liver, and bone metastases and peritoneal carcinomatosis. Therefore, [^{68}Ga]Ga-FAPI PET/CT may lead to significant changes in initial staging when compared to [^{18}F]FDG PET/CT. Another recent study demonstrated that [^{68}Ga]Ga-FAPI-based TNM staging differed in nearly all patients with recurrent/progressive disease compared to staging obtained by contrast-enhanced CT [16]. Therefore, hybrid imaging using FAPI-based tracers may open up new applications in staging and restaging of pancreatic. Moreover, one patient (with widespread metastatic pancreatic cancer) in this study underwent [^{68}Ga]Ga-FAPI PET/CT for the evaluation of therapy response to chemotherapy, which showed an excellent response with decreasing [^{68}Ga]Ga-FAPI activity in most of metastatic lesions. Therefore, we would speculate that [^{68}Ga]Ga-FAPI PET/CT may also be useful for evaluating the treatment response to chemotherapy. The next step is to assess the utility of [^{68}Ga]Ga-FAPI PET/CT in early determination of prognosis in patients with pancreatic cancer. A study addressing this specific question would be an important contribution.

This study has some limitations. First, due to the modest number of patients, we are not able to fully investigate the role of [^{68}Ga]Ga-FAPI PET/CT in clinical management of pancreatic cancer (whether [^{68}Ga]Ga-FAPI PET/CT could modify the clinical management when compared to standard

of care imaging and [^{18}F]FDG PET/CT). Second, more than half of the patients enrolled were in advanced stage and cannot receive surgical resection, and whether [^{68} Ga]Ga-FAPI PET/CT can be beneficial for the staging of pancreatic cancer in earlier stage needs further investigation. Additionally, although dual-time [^{68}Ga]Ga-FAPI PET/CT imaging may help distinguish pancreatitis from malignancy, only six patients underwent dual-time [^{68}Ga]Ga-FAPI PET/CT imaging, and the results are hence preliminary. The hypothesis of differential uptake in pancreatic cancer and pancreatitis should be evaluated in a larger patient cohort.

Conclusions

Compared with [^{18}F]FDG PET/CT, [^{68}Ga]Ga-FAPI PET/CT had a higher sensitivity in the detection of primary tumors, involved lymph nodes, liver/bone metastases, and peritoneal carcinomatosis in patients with pancreatic cancer. As a result, [^{68}Ga]Ga-FAPI PET/CT demonstrated better performance than [^{18}F]FDG PET/CT in terms of TNM staging. The role of [^{68}Ga]Ga-FAPI PET/CT for clinical management in pancreatic cancer requires further investigation.

Supplementary Information The online version contains supplementary material available at https://doi.org/10.1007/s00259-021-05576-w.

Funding This work was funded by the National Natural Science Foundation of China (Grant number 82071963) and the key medical and health projects in Xiamen (Grant numbers 3502Z20191104, 3502Z20209002).

Data availability Data generated or analyzed during the study are available from the corresponding author by request.

Code availability Not applicable.

Declarations

Ethics approval All procedures involving human participants were carried out in accordance with the ethical standards of the institutional and/or national research committee and with the 1964 Helsinki Declaration and its later amendments or comparable ethical standards. This article does not contain any experiments with animals.

Consent to participate Informed consent was obtained from all individual participants included in the study.

Consent for publication Informed consent was obtained from all individual participants included in the study.

Conflict of interest The authors declare no competing interests.

References

1. Siegel RL, Miller KD, Jemal A. Cancer statistics, 2019. CA Cancer J Clin. 2019;69(1):7–34. https://doi.org/10.3322/caac.21551.
2. Li D, Xie K, Wolff R, Abbruzzese JL. Pancreatic cancer. Lancet. 2004;363(9414):1049–57. https://doi.org/10.1016/S0140-6736(04)15841-8.
3. NCCN Guidelines for Pancreatic Adenocarcinoma. Version 2.2021. https://www.nccn.org/professionals/physician_gls/pdf/pancreatic.pdf. Accessed 25 Feb 2021.
4. Strobel O, Buchler MW. Pancreatic cancer: FDG-PET is not useful in early pancreatic cancer diagnosis. Nat Rev Gastroenterol Hepatol. 2013;10(4):203–5. https://doi.org/10.1038/nrgastro.2013.42.
5. Heinrich S, Goerres GW, Schafer M, Sagmeister M, Bauerfeind P, Pestalozzi BC, et al. Positron emission tomography/computed tomography influences on the management of resectable pancreatic cancer and its cost-effectiveness. Ann Surg. 2005;242(2):235–43. https://doi.org/10.1097/01.sla.0000172095.97787.84.
6. Jha P, Bijan B. PET/CT for pancreatic malignancy: potential and pitfalls. J Nucl Med Technol. 2015;43(2):92–7. https://doi.org/10.2967/jnmt.114.145458.
7. Wakabayashi H, Nishiyama Y, Otani T, Sano T, Yachida S, Okano K, et al. Role of 18F-fluorodeoxyglucose positron emission tomography imaging in surgery for pancreatic cancer. World J Gastroenterol. 2008;14(1):64–9. https://doi.org/10.3748/wjg.14.64.
8. Zhang L, Sanagapalli S, Stoita A. Challenges in diagnosis of pancreatic cancer. World J Gastroenterol. 2018;24(19):2047–60. https://doi.org/10.3748/wjg.v24.i19.2047.
9. Yeh R, Dercle L, Garg I, Wang ZJ, Hough DM, Goenka AH. The role of 18F-FDG PET/CT and PET/MRI in pancreatic ductal adenocarcinoma. Abdom Radiol (NY). 2018;43(2):415–34. https://doi.org/10.1007/s00261-017-1374-2.
10. Hamson EJ, Keane FM, Tholen S, Schilling O, Gorrell MD. Understanding fibroblast activation protein (FAP): substrates, activities, expression and targeting for cancer therapy. Proteomics Clin Appl. 2014;8(5–6):454–63. https://doi.org/10.1002/prca.201300095.
11. Siveke JT. Fibroblast-activating protein: targeting the roots of the tumor microenvironment. J Nucl Med. 2018;59(9):1412–4. https://doi.org/10.2967/jnumed.118.214361.
12. Kratochwil C, Flechsig P, Lindner T, Abderrahim L, Altmann A, Mier W, et al. (68)Ga-FAPI PET/CT: tracer uptake in 28 different kinds of cancer. J Nucl Med. 2019;60(6):801–5. https://doi.org/10.2967/jnumed.119.227967.
13. Chen H, Pang Y, Wu J, Zhao L, Hao B, Wu J, et al. Comparison of [(68)Ga]Ga-DOTA-FAPI-04 and [(18)F] FDG PET/CT for the diagnosis of primary and metastatic lesions in patients with various types of cancer. Eur J Nucl Med Mol Imaging. 2020;47(8):1820–32. https://doi.org/10.1007/s00259-020-04769-z.
14. Chen H, Zhao L, Ruan D, Pang Y, Hao B, Dai Y, et al. Usefulness of [(68)Ga]Ga-DOTA-FAPI-04 PET/CT in patients presenting with inconclusive [(18)F]FDG PET/CT findings. Eur J Nucl Med Mol Imaging. 2021;48(1):73–86. https://doi.org/10.1007/s00259-020-04940-6.
15. Nielsen MF, Mortensen MB, Detlefsen S. Key players in pancreatic cancer-stroma interaction: cancer-associated fibroblasts, endothelial and inflammatory cells. World J Gastroenterol. 2016;22(9):2678–700. https://doi.org/10.3748/wjg.v22.i9.2678.
16. Rohrich M, Naumann P, Giesel FL, Choyke PL, Staudinger F, Wefers A, et al. Impact of (68)Ga-FAPI PET/CT imaging on the therapeutic management of primary and recurrent pancreatic ductal adenocarcinomas. J Nucl Med. 2021;62(6):779–86. https://doi.org/10.2967/jnumed.120.253062.
17. Zhao L, Zhuang Y, Fu K, Chen P, Wang Y, Zhuo J, et al. Usefulness of [(18)F]fluorodeoxyglucose PET/CT for evaluating the PD-L1 status in nasopharyngeal carcinoma. Eur J Nucl Med Mol Imaging. 2020;47(5):1065–74. https://doi.org/10.1007/s00259-019-04654-4.

18. Amin MBES, Greene FL, et al. AJCC cancer staging manual. 8th ed. New York, NY: Springer; 2017.
19. Liermann J, Syed M, Ben-Josef E, Schubert K, Schlampp I, Sprengel SD et al. Impact of FAPI-PET/CT on target volume definition in radiation therapy of locally recurrent pancreatic cancer. Cancers (Basel). 2021;13(4). https://doi.org/10.3390/cancers13040796.
20. Wu S, Pang Y, Chen Y, Sun H, Chen H. 68Ga-DOTA-FAPI-04 PET/CT in Erdheim-Chester disease. Clin Nucl Med. 2021;46(3):258–60. https://doi.org/10.1097/RLU.0000000000003491.
21. Wu S, Pang Y, Zhao L, Zhao L, Chen H. 68Ga-FAPI PET/CT versus 18F-FDG PET/CT for the evaluation of disease activity in Takayasu arteritis. Clin Nucl Med. 2021. https://doi.org/10.1097/RLU.0000000000003692
22. Yao L, Zhao L, Pang Y, Shang Q, Chen H. Increased 68Ga-FAPI uptake in ankylosing spondylitis in a patient with rectal cancer. Clin Nucl Med. 2021. https://doi.org/10.1097/RLU.0000000000003798.
23. Zhao L, Pang Y, Sun L, Lin Q, Chen H. Increased 68Ga-FAPI uptake in the pulmonary Cryptococcus and the postradiotherapy inflammation. Clin Nucl Med. 2021. https://doi.org/10.1097/RLU.0000000000003873.
24. Luo Y, Pan Q, Zhang W, Li F. Intense FAPI uptake in inflammation may mask the tumor activity of pancreatic cancer in 68Ga-FAPI PET/CT. Clin Nucl Med. 2020;45(4):310–1. https://doi.org/10.1097/RLU.0000000000002914.
25. Schmidkonz C, Rauber S, Atzinger A, Agarwal R, Gotz TI, Soare A, et al. Disentangling inflammatory from fibrotic disease activity by fibroblast activation protein imaging. Ann Rheum Dis. 2020;79(11):1485–91. https://doi.org/10.1136/annrheumdis-2020-217408.
26. Kamisawa T, Zen Y, Pillai S, Stone JH. IgG4-related disease. Lancet. 2015;385(9976):1460–71. https://doi.org/10.1016/S0140-6736(14)60720-0.
27. Yu X, Zhu W, Di Y, Gu J, Guo Z, Li H, et al. Triple-functional albumin-based nanoparticles for combined chemotherapy and photodynamic therapy of pancreatic cancer with lymphatic metastases. Int J Nanomedicine. 2017;12:6771–85. https://doi.org/10.2147/IJN.S131295.
28. Kang MJ, Jang JY, Chang YR, Kwon W, Jung W, Kim SW. Revisiting the concept of lymph node metastases of pancreatic head cancer: number of metastatic lymph nodes and lymph node ratio according to N stage. Ann Surg Oncol. 2014;21(5):1545–51. https://doi.org/10.1245/s10434-013-3473-9.
29. Sahani DV, Bonaffini PA, Catalano OA, Guimaraes AR, Blake MA. State-of-the-art PET/CT of the pancreas: current role and emerging indications. Radiographics. 2012;32(4):1133–58; discussion 58–60. https://doi.org/10.1148/rg.324115143.
30. Yang J, Zhang J, Lui W, Huo Y, Fu X, Yang M, et al. Patients with hepatic oligometastatic pancreatic body/tail ductal adenocarcinoma may benefit from synchronous resection. HPB (Oxford). 2020;22(1):91–101. https://doi.org/10.1016/j.hpb.2019.05.015.
31. Pery C, Meurette G, Ansquer C, Frampas E, Regenet N. Role and limitations of 18F-FDG positron emission tomography (PET) in the management of patients with pancreatic lesions. Gastroenterol Clin Biol. 2010;34(8–9):465–74. https://doi.org/10.1016/j.gcb.2009.04.014.
32. Low G, Panu A, Millo N, Leen E. Multimodality imaging of neoplastic and nonneoplastic solid lesions of the pancreas. Radiographics. 2011;31(4):993–1015. https://doi.org/10.1148/rg.314105731.
33. Evans DB, Farnell MB, Lillemoe KD, Vollmer C Jr, Strasberg SM, Schulick RD. Surgical treatment of resectable and borderline resectable pancreas cancer: expert consensus statement. Ann Surg Oncol. 2009;16(7):1736–44. https://doi.org/10.1245/s10434-009-0416-6.
34. Zhao L, Pang Y, Luo Z, Fu K, Yang T, Zhao L, et al. Role of [(68)Ga]Ga-DOTA-FAPI-04 PET/CT in the evaluation of peritoneal carcinomatosis and comparison with [(18)F]-FDG PET/CT. Eur J Nucl Med Mol Imaging. 2021;48(6):1944–55. https://doi.org/10.1007/s00259-020-05146-6.
35. Alberts I, Sachpekidis C, Dijkstra L, Prenosil G, Gourni E, Boxler S, et al. The role of additional late PSMA-ligand PET/CT in the differentiation between lymph node metastases and ganglia. Eur J Nucl Med Mol Imaging. 2020;47(3):642–51. https://doi.org/10.1007/s00259-019-04552-9.
36. Mei R, Allegri V, Calabro D, Fanti S, Ambrosini V. Delayed imaging with oral contrast improves [68Ga]Ga-DOTANOC PET/CT detection of primary duodenal neuroendocrine tumor (NET). Eur J Nucl Med Mol Imaging. 2021;48(5):1684–5. https://doi.org/10.1007/s00259-020-05138-6.
37. Hoffmann MA, Buchholz HG, Wieler HJ, Rosar F, Miederer M, Fischer N et al. Dual-time point [(68)Ga]Ga-PSMA-11 PET/CT hybrid imaging for staging and restaging of prostate cancer. Cancers (Basel). 2020;12(10). https://doi.org/10.3390/cancers12102788.

Authors and Affiliations

Yizhen Pang[1] · Long Zhao[1] · Qihang Shang[1] · Tinghua Meng[1] · Liang Zhao[2] · Liuxing Feng[3] · Shuangjia Wang[3] · Ping Guo[3] · Xiurong Wu[4] · Qin Lin[2] · Hua Wu[1] · Weipeng Huang[5] · Long Sun[1] · Haojun Chen[1]

1 Department of Nuclear Medicine & Minnan PET Center, Xiamen Cancer Center, The First Affiliated Hospital of Xiamen University, Teaching Hospital of Fujian Medical University, Xiamen, China

2 Department of Radiation Oncology, Xiamen Cancer Center, The First Affiliated Hospital of Xiamen University, Teaching Hospital of Fujian Medical University, Xiamen, China

3 Department of Hepatobiliary & Pancreatovascular Surgery, The First Affiliated Hospital of Xiamen University, Teaching Hospital of Fujian Medical University, Xiamen, China

4 Department of Radiology, The First Affiliated Hospital of Xiamen University, Teaching Hospital of Fujian Medical University, Xiamen, China

5 Department of Nuclear Medicine, Jieyang Affiliated Hospital, Sun Yat-Sen University, Jieyang, China